Development of a Superconducting Magnet for a Compact Cyclotron for Radioisotope Production

Luis García-Tabarés, Pablo Abramian, Jesús Calero, José L. Gutiérrez, Javier Munilla, Diego Obradors, Jose M. Perez, Fernando Toral, Rafael Iturbe, Leire Mínguez, José Gómez, Elena Rodilla, Marta Bajko, Matthias Michels, Daniel Berkowitz, and Friedrich Haug

***Abstract*—The present paper describes the development process of a low critical temperature superconducting magnet to be installed in a compact cyclotron producing single-dose radioisotopes for clinical and preclinical applications. After a brief description of the accelerator, the magnet development process is described, starting from the magnetic, mechanical, quench, and thermal calculations, continuing with the designing process, particularly the support structure of the magnet and the cryogenic supply system, to finish with the fabrication and the first tests than have been performed.**

***Index Terms*—Compact cyclotrons, cryogenics, magnet, radioisotope, superconducting.**

I. Introduction

POSITRON Emission Tomography (PET) has been demonstrated to be one of the most efficient molecular imaging techniques for clinical and preclinical needs. 90% of the PET clinical scans are currently performed with the isotope ^{18}F due to the suitability of the fludeoxyglucose (FDG) radiotracer for a vast number of applications. In the last years, other tracers have also been considered, including those based on ^{11}C, like Methionine, Choline or others [1].

The delivery of FDG in large central production centers has been demonstrated to be a cost-effective solution for populated areas, but the interest on other PET isotopes and tracers has raised expectations that cannot be satisfied by using the concept of large central production centers [2].

A new production method capable of providing single doses of the desired isotope would satisfy the requisites for non-standard PET demands. This method is based on the use of an accelerator providing the minimum required energy and current, with a reduced footprint [3].

Manuscript received October 15, 2015; accepted March 15, 2016. Date of publication March 29, 2016; date of current version April 22, 2016. This work was supported in part by the Spanish Center for Industrial and Technological Development under Project CEN-20101014 and in part by the EuCARD-2 collaboration, which is cofunded by the partners and the European Commission under Capacities Seventh Framework Programme under Grant 312453.

L. García-Tabarés, P. Abramian, J. Calero, J. L. Gutiérrez, J. Munilla, D. Obradors, J. M. Perez, and F. Toral are with CIEMAT, 28040 Madrid, Spain (e-mail: luis.garcia@ciemat.es).

R. Iturbe and L. Mínguez are with ANTECSA, 48920 Portugalete, Spain.

J. Gómez and E. Rodilla are with The Vacuum Projects, 46988 Paterna, Spain.

M. Bajko, M. Michels, D. Berkowitz, and F. Haug are with Conseil Européen pour la Recherche Nucléaire (CERN), 1211 Geneva, Switzerland.

Color versions of one or more of the figures in this paper are available online at http://ieeexplore.ieee.org.

Digital Object Identifier 10.1109/TASC.2016.2548429

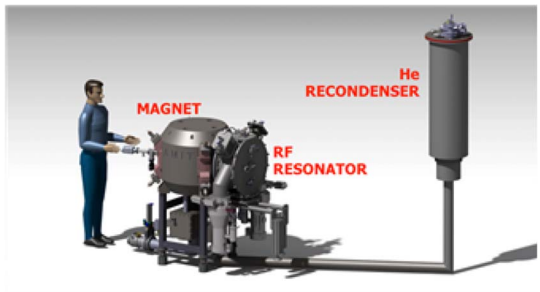

Fig. 1. General arrangement of the AMIT cyclotron.

From this background, the AMIT project (Advanced Molecular Imaging Technologies) was started in the year 2010, a multilateral collaboration of Spanish institutes and industries, led by SEDECAL and funded in the framework of a governmental program in which some foreign contributions, like CERN, were also included.

II. The AMIT Cyclotron

One of the goals of the AMIT project is to develop a compact cyclotron for single dose production of ^{18}F and ^{11}C. It is Lawrence type machine accelerating H^- up to an energy of 8.5 MeV and a current of 10 μA [4].

Since, for a given energy, the product of the cyclotron extraction radius times the magnetic field density is constant, the only way for reducing the sizes of the accelerator is by increasing its magnetic field using a superconducting magnet. In this case, it is a NbTi magnet which is cooled down with two-phase helium, circulating in a closed circuit and recondensed externally. Fig. 1 depicts the general arrangement of the AMIT system.

III. The Magnetic Circuit

The magnetic circuit of the AMIT Cyclotron includes two superconducting coils in a Helmholtz arrangement and the magnetic iron yoke, which configures the precise required vertical field in the accelerating chamber and acts as a return flux path, minimizing stray fields. It is a warm iron configuration, where only the coils are kept cold inside a common cryostat.

Table I shows some basic parameters of the cyclotron superconducting magnet.

TABLE I
CYCLOTRON SUPERCONDUCTING MAGNET PARAMETERS

Parameter	Value
Magnetic Central Field	4.00 T
Magnetic Field Radial Gradient @ r=105 mm	1.49 %
Nominal Current	108.6 A
Working Point in the Load Line @ 4.2 K/4.7K	70.5/76.5 %
Self Inductance (Both Coils) @ Nom. Current	38.35 H
Insulated wire diameter	0.896 mm
Cu/Sc	4.5:1

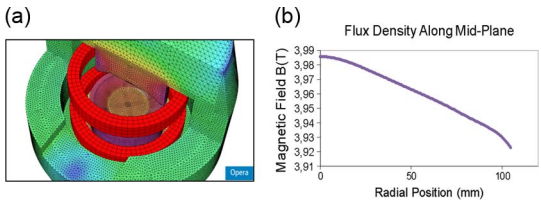

Fig. 2. (a) Opera magnetic modeling. (b) Radial magnetic field distribution.

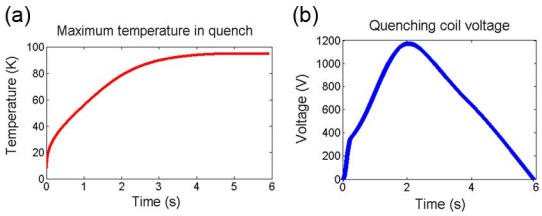

Fig. 3. (a) Temperature and (b) voltage after a coil quench.

Initial magnetic design, aims at minimizing the overall magnet volume, while satisfying the corresponding field accuracy and shape requirements, which include a given radial field gradient to achieve beam focusing.

Magnetic design started by defining the field in the magnet center. Once the superconducting material was chosen, a simplified optimization process was developed to find a field value that minimized the overall weight of the magnet. It was found that the minimum value was located around 4 T, which was finally the selected value.

Since the space required for the vacuum chamber breaks the iron axial symmetry, the first magnetic calculation were made based on a pseudo-3D model (2D QuickField FEM code using azimuthally averaged permeabilities) which was then refined running actual 3D models in Opera [5]

Fig. 2(a) shows the radial field distribution, while Fig. 2(b) shows the preliminary 3D Opera model to compute it. The model is also used to check that the stray field specification is fulfilled.

Also quench simulation for this final design has been carried out using custom-made software based in Matlab [6]. Fig. 3 shows the results for the temperature evolution of the hot spot and the maximum voltage appearing at the quenched coil.

Superconducting coils must support high magnetic radial and vertical forces that can lead to mechanical damage or deformations affecting the field quality [7]. To reduce the effects of radial forces, coils include an outer aluminum shrink-fitted cylinder that induces azimuthal compressive stresses in the coil, compensating those induced by electromagnetic forces.

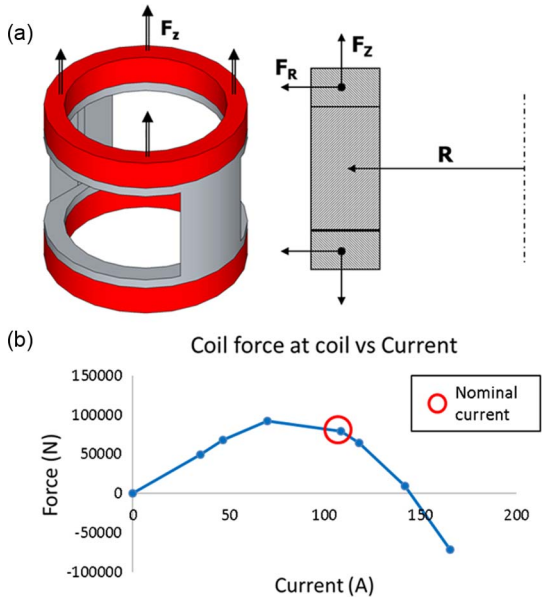

Fig. 4. (a) Schematic of forces in the coil. (b) Vertical force calculation.

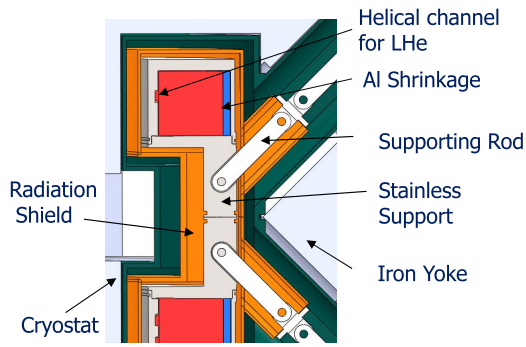

Fig. 5. Coil, crsyostat, and support structure cross section.

Although the net vertical force of the two coils is null under nominal conditions, individual forces acting on them can be very high. These forces arise from the interaction between both windings and between the coils and the iron. Coils need to share a common structure to avoid transferring those forces to the cryostat.

This annular structure also acts as a coil casing and must include an aperture to allow inserting the cyclotron vacuum chamber through it. It also includes a helical channel to allow the circulation of the two-phase helium. Fig. 4(a) shows the forces acting on the coils and Fig. 4(b) the calculated values for the vertical forces versus the coil current (positive values for repulsive forces and negative values for attractive forces). At high current values, repulsive forces between coil and iron get higher and so, the net magnetic force over each single coil switches its sign (see Fig. 5).

The coils and the casing are inserted in a cryostat, which includes a radiation screen to minimize thermal losses to liquid helium. To withstand the weight of the system (around 220 kg including the coils and casing) and also to adjust its position with respect to the iron, a high stiff concept support has been developed, based on the use of Cryogenic Grade Glass Fiber

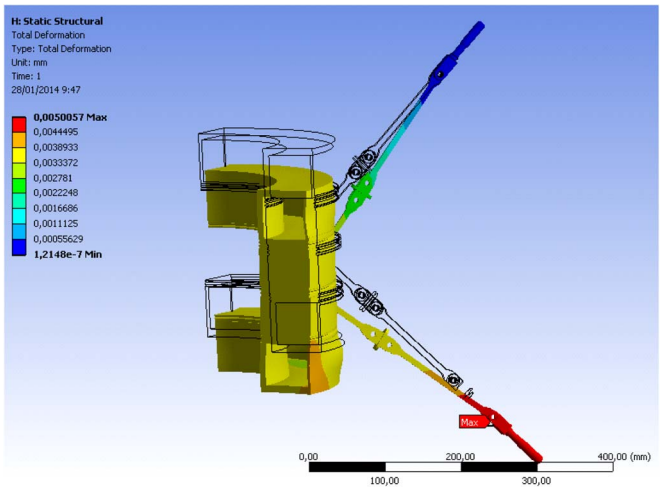

Fig. 6. Structural model of mechanical behavior of the rods, including weights, magnetic forces, temperatures, and mechanical joints.

Reinforced Polymer (GFRP-CR) rods due to its low thermal conductivity.

The structure includes 8 rods, 4 in its upper part, which are really in charge of withstanding the system weight, and another 4 in the lower part to improve lateral stiffness, and also to compensate forces arising from the misalignment between the coil and the iron axes, which could be up to 0.5 mm in any direction.

Rods are also needed to achieve secure operation if vertical forces appear in the upward direction since these rods are designed only for traction operation avoiding bending or compression. For the mechanical design, a new complete model including magnetic forces and thermomechanical stresses was developed using Ansys and Maxwell (Fig. 6).

The radiation screen and the current leads are refrigerated using gas helium. Both, liquid and gas helium are provided by a Cryogenic Supply System (CSS) that will be described in Section IV. Helium is transferred from the CSS through a low-loss Transfer Line that is connected to the Cyclotron Connection Box, a built-in device that provides space, electrical insulation and thermal refrigeration for the current leads, instrumentation and all the safety valves for the whole fluid circuit. It also allows different refrigeration configurations like supplying LHe directly from a Dewar instead of from the CSS.

Main contributions to the heat losses are radiation and conduction. Regarding radiation and in order to reduce the heat adsorbed by the casing, a refrigerated thermal shield is covering the whole casing and any other part at liquid helium temperature, including the casing, the connection box and connecting pipes. A reflective adhesive layer is added to the external surface of the casing to reduce emissivity while improving surface reflectiveness. The refrigeration of this thermal shield is done from the helium gas supplied by the CSS.

Conduction heat losses mainly come from the supporting rods of the casing as mentioned before. These rods have been split in two parts and the joint intercepted with the thermal shield to reduce, even more, heat losses to liquid helium

High Temperature Superconductive current leads have been selected to reduce conduction losses as well as heat generation

TABLE II
THERMAL LOSSES CALCULATION

Contributions	Value (W)
LOADS @ 4.5 K	
Cyclotron	0.53
Connection Box	0.16
Total at 4,5 K	**0.70**
LOADS @ Cryocooler First Stage	
Thermal Shield	10
Current Leads	10.5
Connection Box	4
Others	9.5
Total at First Stage	**34**

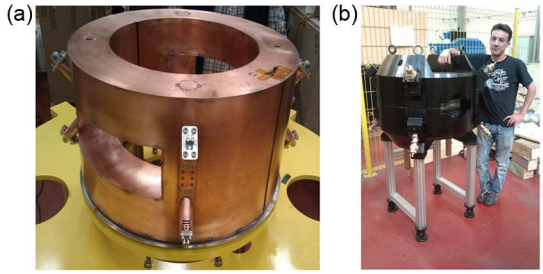

Fig. 7. Magnet manufacturing. (a) Thermal shield assembled around the casing and (b) quality measurements during cryostat assembly.

from the current supply. Some other heat losses coming from the safety parts (pipes, valves, etc. . .) have also been reduced, using a thermal interception procedure. A chart including the final heat losses at both stages for all contributions can be found in Table II.

Magnet component fabrication has been performed by several companies according to their different expertise: *ANTECSA* for the superconducting coils and the iron, *The Vacuum Projects* for the cryostat and radiation screen also in collaboration with *ANTECSA* and CIEMAT for integration, including the connection box. Previously to final manufacturing some prototypes or dummies were done for validating different procedures. Fig. 7 shows two different stages of the magnet fabrication process.

IV. MAGNET COOLING SYSTEM

As explained in Section III, both coils of the magnet are cooled at 4.5 K with evaporating liquid helium circulating through helical channels along the inner wall of the coil casing. Ideally the coolant enters the channels in liquid phase. However, also two-phase flow arriving from the refrigeration system can be accepted as long as the exit flow contains liquid to maintain isothermal conditions of the magnet. This condition along with the thermal loss inventory has been used to dimension the magnet cooling channel. [8]

The non-isothermal cooling of the thermal shield of the coils and the cryostat and also the magnet current leads is done with a helium gas flow at 30 to 60 K.

Both flows are supplied by the same device, the Cryogenic Supply System (CSS). As cold sources for both liquid and gas flows, a two-stage GM cryocooler is used with a rated cooling power of 1.5 W at 4.2 K [9].

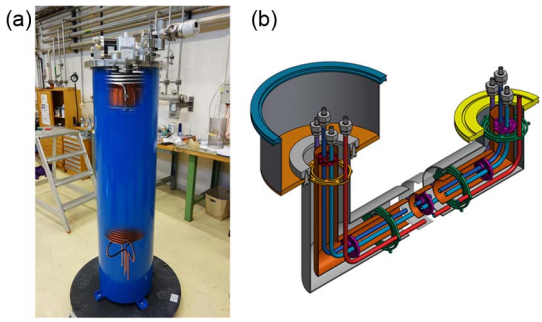

Fig. 8. (a) Cryogenic supply system. (b) Low-loss transfer line.

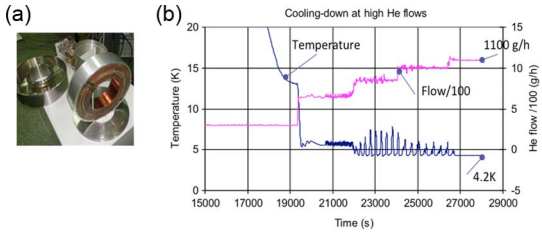

Fig. 9. (a) Cold arrangement in the single coil test. (b) Measurements of the required cooling flow.

Basically the CSS is a closed pumped helium circuit. The fluid is first cooled down from ambient temperature to around 30 K and then directed to the thermal shielding circuits. The flow is then returned to the CSS again and re-cooled to 4.5 K and condensed. The liquid exits the CSS and is sent to the cooling channels of the coils. Then this flow is returned to the CSS. The overall configuration of the CSS consists of a number of heat exchangers and "thermal anchorings" to the two stages of the cryocooler.

The CSS system is installed inside a vacuum vessel. A specially designed low-loss helium transfer line links the CSS with the magnet cryostat for remote cooling, entering in the connection box of the cyclotron. Fig. 8(a) shows a picture of the CSS in which a rendering of one of the heat exchangers has been included for clarification. Fig. 8(b) shows a conceptual drawing of the Transfer Line.

The CSS has been fully validated in stand-alone operation. For this the coils' fluid channels and the coil's thermal loads can be simulated with a purpose designed "validator system" which is installed in a test cryostat. Results are in good agreement with expectations; experimentally a maximum cooling power of 1.3 W at 4.5 K could be measured.

V. Ongoing Experimental Results

In order to validate magnetic, mechanical and thermal concepts, a first test was performed (the Single Coil Test [10]) with a similar coil to the real ones but with half diameter, approximately. Refrigeration principle was the same and helium was provided from a pressurized Dewar. Helium flow mass could be controlled and measured and the radiation screen was cooled down using liquid nitrogen. Fig. 9 (left) shows the coil arrangement, including the shrinking aluminum cylinder and the casing. Basically two were the aims of the test: measuring the required flow to keep the magnet cold at 4.2 K and performing the training of the coil in spite of quite different magnetic conditions than the real ones. In both cases, comparison with predictions was crucial to validate the models for the actual cyclotron magnet. Regarding the training tests, the coil performed extremely well achieving short-sample critical current without any premature quench. With respect to the flow mass, it was in very good agreement with the predicted values from the calculated losses. Fig. 9 (right) is a plot showing the required minimum flow of helium to keep the magnet at 4.2 K

After finishing the real cyclotron coils, they were tested at CERN in a vertical cryostat by immersion in a liquid helium bath and trained and re-trained after warming them up. Main conclusions were that they went all beyond equivalent nominal current without training and that they didn't show a significant re-training.

VI. Conclusion

There is a significant and increasing interest in compact small cyclotrons for single dose production of different radioisotopes. The only way for reducing the footprint of this kind of accelerators is increasing its magnetic field using superconducting magnets. We have presented in this work the design calculation of a superconducting magnet for a compact cyclotron, which includes magnetic computations, mechanical calculations, quench studies and thermal analysis to define the heat loss inventory. Design considerations are also presented, especially those concerning the coil supporting structure and the connection box as well as some comments on the system fabrication and integration.

Finally, some preliminary experimental results are shown, including those achieved in a test where a smaller coil working under the same principle was magnetically and mechanically tested, with very encouraging results, and also the first training results of the actual cyclotron coils.

References

[1] "FDA approves 11C-Choline for PET in prostate cancer," U.S. Food Drug Admin., Silver Spring, MD, USA, May 2014. [Online]. Available: jnm.snmjournals.org

[2] U. Zetterberg, "A change in usage of cyclotrons for medical isotope production?" presented at the Compact Accelerators for Isotope Production Workshop, Mar. 26–27, 2015, Cockcroft Institute, Daresbury, U.K.

[3] D. M. Lewis, "World market usage and industrial production," presented at the The Cockcroft Institute, Daresbury, U.K., 2011. [Online]. Available: https://eventbooking.stfc.ac.uk/uploads/accelerator_driven_production_of_medical_isotopes/dewi-lewis-20111204-dml-workshop-markets-etc.pdf

[4] C. Oliver *et al.*, "Optimizing the radioisotope production with a weak focusing compact cyclotron," in *Proc. Cyclotrons*, Vancouver, BC, Canada, 2013, pp. 429–431.

[5] F. Toral, "The AMIT cyclotron magnet," in *Proc. Panel Rev. Meet.*, Madrid, Spain, 2012, pp. 5–8.

[6] F. Toral, "Design and calculation procedure for particle accelerator superconducting magnets: Application to an LHC superconducting quadrupole," Ph.D. dissertation, Dept. Electr. Eng., Univ. Pontificia de Comillas (UPCO), Madrid, Spain, 2001.

[7] Y. Iwasa, *Case Studies in Superconducting Magnets: Design and Operational Issues*. New York, NY, USA: Springer-Verlag, 2009.

[8] R. F. Barron, *Cryogenic Heat Transfer*. Philadelphia, PA, USA: Taylor & Francis, 1999.

[9] F. Haug, "The AMIT magnet cryosystem," in *Proc. Panel Rev. Meet.*, Madrid, Spain, Nov. 2012, pp. 14–16.

[10] J. Munilla *et al.* "Validation test of the forced-flow cooling concept for the superconducting magnet of AMIT cyclotron," *IEEE Trans. Appl. Supercond.*, vol. 26, no. 3, Jun. 2016, Art. no. 4401204.